Synthesis of Composite Hydrogels Incorporating D,L-Cyclic Peptide Nanotubes as a Platform for Materials Engineering

by

Pei Kun Richie Tay

B.S. Chemical and Biomolecular Engineering
Johns Hopkins University, 2008

Submitted to the Health Sciences and Technology Program
in Partial Fulfillment of the Requirements for the Degree of

Master of Science in Health Sciences and Technology

at the

Massachusetts Institute of Technology

September 2012

Signature of Author: _____
Health Sciences and Technology Program
September 4, 2012

Certified by: _____
Neel Joshi
Assistant Professor of Chemical and Biological Engineering, Harvard University
Thesis Supervisor

Accepted by: _____
Arup Chakraborty
PhD. Director, Institute for Medical Engineering and Sciences
Robert T. Haslam Professor of Chemical Engineering, Chemistry and Biological Engineering,
Massachusetts Institute of Technology

DISCLAIMER

MISSING PAGE(S)

There are some pagination issues with this thesis. This is the most complete version available.

Synthesis of Composite Hydrogels Incorporating D,L-Cyclic Peptide Nanotubes as a Platform for Materials Engineering

by

Pei Kun Richie Tay

Submitted to the Health Sciences and Technology Program
On September 4, 2012 in Partial Fulfillment of the Requirements for the Degree of Master of Science in Health Sciences and Technology

Abstract

Composite hydrogels find increasing use as biomaterials because the addition of a filler often improves on the material properties of the original matrix, or provides new optical, magnetic, conductive or bioactive functionalities not inherent to the hydrogel. In this work we synthesized nanocomposite gelatin methacrylate (GelMA) hydrogels that incorporate D,L-cyclic peptide nanotubes. These nanotubes are biocompatible, stiff and their physical and chemical properties can be tailored simply by changing the amino acid sequence of the peptide. We show that the nanotubes successfully integrated into the hydrogel matrix and provided some mechanical reinforcement, without affecting hydrogel porosity or hydration characteristics. We will be using this composite system as a platform for engineering hydrogels with unique physical and biological properties to the hydrogel, for application as biological scaffolds.

Thesis Supervisor: Neel Joshi
Title: Assistant Professor of Chemical and Biological Engineering, Harvard University

Acknowledgements

I would like to thank Prof. Joshi for his kind words, patient guidance and helpful feedback throughout the shaping and execution of this project. All members of the lab contributed in some capacity, but special thanks to Dr. Peter Nguyen for help with peptide synthesis and SEM imaging. I would also like to thank Dr. Akhilesh Gaharwar from the Khademhosseini Lab for advice on hydrogel synthesis and characterization. This work would not have been possible without the resources and technical staff at the Wyss Institute at Harvard University, and generous administrative support from the Harvard-MIT Division of Health Sciences and Technology. Finally, I would like to thank my family for their love and encouragement, which has carried me through many long hours in the lab.

Table of Contents

List of Figures

List of Abbreviations

4-Dimethylaminopyridine (DMAP)
N,N'-diisopropylcarbodiimide (DIC)
2-(6-Chloro-1H-benzotriazole-1-yl)-1,1,3,3-tetramethylaminium hexafluorophosphate) (HCTU)
Diisopropylethylamine (DIEA)
Triisopropylsilane (TIPS)
Hydroxybenzotriazole (HOBt)
7-azabenzotriazol-1-yloxy)tripyrrolidino-phosphonium hexafluorophosphate (PyAOP)
Trifluoroacetic acid (TFA)
Dimethylformamide (DMF)
Dichloromethane (DCM)
Cyclo-[(Glu-*D*-Ala)$_4$] (EA_4)
Poly(ethylene glycol) (PEG)
Gelatin methacrylate (GelMA)

1. Introduction

1.1 Peptide nanotubes

1.1.1 Self-assembling peptide systems

Tubular protein aggregates are widespread in nature; they range from actin filaments within cells; to viral capsids, bacterial flagella[1] and biofilm curli fibers;[2] to prions and amyloid proteins involved in degenerative diseases. Because nanotubes and filaments are useful in fields as varied as molecular transport, optics, catalysis, electronics, drug delivery and biosensing, much attention has been paid towards replicating the tubular structure of protein polymers in a controlled fashion. Since proteins are complex biomolecules and inherently difficult to engineer and produce in bulk, researchers have instead focused on model peptides inspired by an understanding of protein self-assembly.

The smallest of these building blocks are dipeptides of phenylalanine (FF), a motif derived from the Alzheimer's β-amyloid protein.[3] The FF peptide assembles by a combination of hydrogen bonding and π-π stacking of the Phe side chains to form multi-walled nanotubes that are remarkably stiff (Young's modulus ~19 GPa).[4] Slightly longer peptide amphiphiles pioneered by Shuguang Zhang, comprising one or two charged head residues and a tail of hydrophobic residues (e.g. A_6D, L_6DD), form hydrogen-bonded β-sheet bilayers that wrap around to create hollow nanotubes.[5] Similar surfactant-like peptide designs that incorporate longer alkyl chains were also employed by Matsui et al.[6] and the Stupp lab[7] to create tubular peptide assemblies.

1.1.2 Self-assembling D,L-cyclic peptides

De Santis et al. first proposed that cyclic peptides containing an even number of alternating D- and L-amino acids would stack to form β-sheet-like structures,[8] but it was Ghadiri and co-workers who successfully assembled and imaged these D,L-cyclic peptide (DLCP) nanotubes.[9] The stereochemistry of the cyclic backbone forces the amide N-H and C=O bonds to align parallel to the tube length (thus creating the hydrogen bonded network that stabilizes the tubes), while amino acid side chains project axially. This arrangement opens several avenues for customization of nanotube properties that are not open to the linear systems described above. For instance, tube diameter is easily controlled by varying the number of residues in the backbone, or by adding chiral β^3-amino acid residues.[10,11] The geometry and hydrophobicity of tube interior could also be altered by incorporating γ- or ε-amino acids.[12-14] These non-natural residues contribute other material enhancements: Nanotubes comprised entirely of β-amino acids adopt a parallel β-sheet formation (distinct from the antiparallel formation of α-DLCPs), with a distinct tubular dipole that is useful for ion transport applications,[11] while the use of γ-amino acids gives rise to more rigid tubes because the cyclic γ-residue helps to rigidify the peptide backbone.[15] Since the outer surface is defined by the amino acid side chains, external functionality could be altered simply by changing the amino acid sequence, which would be useful when contemplating nanotube assembly conditions or chemical conjugation of other moieties. Finally, nanotube

assembly could be capped using N-methylated residues,[16] and tubes could also be stapled via side chain residues.[17]

1.1.3 D,L-cyclic peptide nanotubes as templates in biomaterials engineering

With prudent peptide design, the properties of DLCPs can easily be tailored to suit a variety of applications. A large proportion of past and current DLCP research has focused on the ability of these peptides to form membrane pores or channels. Inserted into bacterial membranes, these tubular channels proved to be effective antibacterial agents,[18] but they have also shown utility for the transport for ions,[19] glucose[20] and amino acids,[21] and also as effective ion sensors.[22]

Other applications exploit the regular array of functional groups on the outer surface of the nanotubes, which can be used for small molecule conjugation or for the templating of larger macromolecules. For example, Ghadiri's group coupled 1,4,5,8-naphthalenetetracarboxylic diimide (NDI) to Lys residues, and showed that self-assembly of the tubes was accompanied by the alignment of NDI groups to create charge-delocalized states, which might potentially be useful for creating molecular electronic devices.[23] By introducing negatively-charged side groups, or conjugating metal-binding moieties to amino acid side chains, tubes could also be used to nucleate the deposition of metals to create nanowires.[24-26] Further, artificial photosystems could be engineered using heterodimeric nanotubes bearing electron-donor units (e.g. exTTF) and photoactive electron-acceptor units (e.g. C_{60}).[27] Finally, Biesalski and coworkers added initiator groups to the side chains, and used the assembled tubes as a template to create polymeric shells.[28,29]

We feel that there is a gap in the literature for the use of DLCP nanotubes in biomaterials development for biomedical research. The versatility in peptide design, combined with the flexibility of introducing a variety of biomedically relevant functionalities, would make cyclic peptide nanotubes ideal candidates as components of biological scaffolds, hence our choice to work with these peptides in this project.

1.2 Composite hydrogels

1.2.1 Nanocomposite hydrogel systems

Hydrogels are swollen crosslinked polymer networks used extensively in biomedicine for drug delivery, tissue engineering, biosensing and as coatings for devices. Composite hydrogel systems contain a second component, usually added to compensate for deficits in the original hydrogel (e.g. to bolster gel mechanical strength) or to introduce application-specific material properties. The latter could include conductivity (with the addition of carbon nanotubes);[30,31] magnetic properties (by adding iron oxide particles);[32,33] improved thermal and mechanical stability (with silicates, clay or nanotubes);[34-37] bioactivity (e.g. hydroxyapatite crystals to simulate bone);[38-40] or the capacity for remote actuation (e.g. iron oxide ferrogels that are heated by near-infrared light to release a drug cargo).[41]

1.2.2 Nanotube fillers in nanocomposite hydrogels

Nanofibrous and nanotubular fillers are popular in composite hydrogel systems because their high aspect ratio maximizes filler-matrix contact and thus reduces interfacial material defects.[42] Biologically-derived chitin and cellulose nanowhiskers find increasing use as hydrogel stiffening fillers,[34,35,43-45] although carbon nanotubes (CNTs) remain the most extensively studied for their ability to impart both mechanical reinforcement and conductive properties to weak hydrogels. There are many disadvantages to the use of carbon nanotubes in biological scaffolds, including their strong hydrophobicity and limited dispersibility in physiological media; the difficulty in producing CNTs with precise structural properties; and their chemical inertness, with limits their capacity for biofunctionalization. DLCPs, however, share many of the properties of CNTs and polysaccharide-based nanotubes, but have an inherently larger design space for incorporating a range of material properties.

1.3 Specific aims

Our main goal was to create nanocomposite hydrogels that incorporated DLCP nanotubes. This involved (1) designing a cyclic peptide that would interact with the hydrogel matrix; (2) selecting a hydrogel system that would accommodate and stabilize the peptide nanotubes; and (3) characterizing the nanocomposite hydrogel to ensure functional integration of the nanotubes within the matrix.

Aims 1 and 2 were pursued in parallel to ensure that the properties of the peptide complemented those of the hydrogel; for instance, if we chose a peptide with predominantly hydrophobic residues, we wanted a gel polymer with hydrophobic domains that would interact with those residues. Our choice of peptide was also influenced by its amenability towards chemical modification, since we would eventually be introducing various chemical groups to add functionality to the nanocomposite. We briefly contemplated assembling the nanotubes within the hydrogel, either prior to or post-polymerization, but this was disadvantageous in several ways, including the presence of steric and diffusion constraints that might adversely affect assembly, and the inability to control the assembly process to obtain nanotubes of specific dimensions. Instead, we opted to assemble the peptide nanotubes separately so that we can investigate their properties and their stability under specific gelation conditions.

For Aim 2, we looked for biocompatible and bioactive polymers to ensure that our platform was broadly applicable for biological studies. We also considered only fast-gelling systems (i.e. gelation within minutes) to ensure that the peptide nanotubes remained evenly dispersed during the creation of the nanocomposite hydrogel.

Characterization studies in Aim 3 focused on determining the distribution of the nanotubes in the hydrogel, how they were interacting with the gel polymer, and how this interaction affected the physical properties of the gel. Since the nanotubes were stiff fillers, we looked at how their presence influenced gel mechanics via compression and dynamic oscillatory tests. We also examined the effect of nanotube concentration on the porosity and hydration properties (and thus the internal environment) of the composite gels.

2. Peptide synthesis and nanotube assembly

2.1 Introduction: Choice of cyclic peptide

We considered the following properties when choosing the cyclic peptide sequence for our study: (1) the peptide should contain residues that stabilize it within the hydrogel matrix of choice; (2) the peptide should have residues that can be functionalized to introduce additional properties, but not at the expense of nanotube assembly; (3) assembled nanotubes should have a large aspect ratio to increase interaction with the hydrogel; and (4) the nanotubes should be stable in aqueous media and under the conditions of gelation. Cyclo-[(Glu-*D*-Ala)$_4$] (abbreviated EA$_4$) satisfied all of these criteria. The glutamic acid side chain could interact with a variety of hydrophilic and anionic polymers, and is useful for bioconjugation. Further, peptides with a similar sequence—cyclo-[(Glu-*D*-Leu)$_4$] (QL$_4$), cyclo-[(Gln-*D*-Ala)$_4$] (EL$_4$), cyclo-[(Gln-*D*-Ala-Glu-*D*-Ala)$_2$] (QAEA$_2$)—are known to form long tubular crystals that can be stably dispersed in water.[9,26,46,47]

Hartgerink previously assembled EL$_4$ using a vapor equilibration method.[26] The peptide was dissolved at basic pH and floated in a vessel filled with neat TFA; as the aqueous solution acidified, the Glu side chains (pK_a ~4.1) ceased to repel each other electrostatically, allowing the peptide monomers to assemble into tubes over several days. The symmetry of the cyclic peptide and hydrogen bonding between the Glu carboxylates led individual tubes to crystallize into aggregates several hundred nanometers in width and tens of microns in length. While these microcrystals are well-defined, their large size could prevent proper interfacing with the hydrogel matrix and also reduce pore sizes. We used similar pH-triggered assembly conditions for EA$_4$, but we added TFA directly to the peptide with stirring to limit crystallization.

2.2 Materials and methods

2.2.1 Solid state peptide synthesis

2.2.1.1 General

Wang resin was purchased from Novabiochem. 4-Dimethylaminopyridine (DMAP), hydroxybenzotriazole (HOBt), and Fmoc amino acids were purchased from APPTec USA. 2-(6-Chloro-1H-benzotriazole-1-yl)-1,1,3,3-tetramethylaminium hexafluorophosphate) (HCTU) was purchased from P3 BioSystems. 7-azabenzotriazol-1-yloxy)tripyrrolidino-phosphonium hexafluorophosphate (PyAOP) and triisopropylsilane (TIPS) were purchased from Oakwood Chemicals. Tetrakis(triphenylphosphine)palladium(0) was purchased from Strem Chemicals. Trifluoroacetic acid (TFA) and acetic anhydride were purchased from J.T. Baker. HPLC-grade dimethylformamide (DMF), dichloromethane (DCM), methanol, acetonitrile and diethyl ether were purchased from Fisher. Piperidine, diisopropylethylamine (DIEA) and remaining reagents and solvents were purchased from Aldrich. DMF and DCM were dried over 4 Å molecular sieves; all other reagents and solvents were used as received.

Peptides were synthesized using standard Fmoc chemistry on Wang resin in a glass vessel. On-resin cyclization was modified from the strategy of Rovero et al.,[48] with the first

residue—Fmoc-*L*-Glu(OAll)—attached to the resin via the β-carboxylate group. LC/MS spectra were obtained using an Agilent 1290/6140 LC/MS system (1290 Infinity LC instrument coupled to 6140 Quadrupole MSD system) on a C_{18} column. NMR spectra were obtained on the Varian 400 MHz MR spectrometer.

2.2.1.2 Resin loading

Wang resin was swollen in 9:1 v/v DCM:DMF for 1 hr. Four equivalents (relative to resin) each of Fmoc-Glu(OAll) and HOBt were dissolved in the same solvent mixture and added to the resin, followed by 0.2 eq. of DMAP (dissolved in DMF) and 4 eq. of DIC. The mixture was agitated with a mechanical shaker for 5 hr, then 2 eq. of acetic anhydride and pyridine was added and mixed for 30 min to cap all unreacted hydroxyl groups. The resin was washed sequentially three times with DMF, DCM and methanol, and dried overnight *in vacuo*. We quantified resin loading using Fmoc release based on an established protocol.[49]

2.2.1.3 Peptide synthesis

Fmoc-Glu(OAll) Wang resin (1 g) was swelled in 1:1 v/v DMF:DCM for 1 hr. Fmoc deprotection was carried out using 25% v/v piperidine/DMF (3 x 5 min). The resin was then washed with DCM and DMF (3 x 1 min), and deprotection confirmed using the ninhydrin-based Kaiser test. A solution of Fmoc-amino acid, HCTU (both 4 eq. relative to resin) and DIEA (8 eq.) in 1:1 v/v DMF:DCM was allowed to pre-react for 5 min, then added to the resin. After shaking for 15 min, the resin was washed and coupling confirmed using the Kaiser test as above. A second round of coupling was performed if the Kaiser test was positive. We repeated the deprotection/cycling cycle to obtain the linear peptide.

Before cyclizing the peptide, we first hydrolyzed the allyl ester protecting group. The resin was washed thrice with degassed DCM, then phenylsilane (25 eq. in degassed DCM) was added and mixed with the resin for 5 min. Next, tetrakis(triphenylphosphine)palladium(0) (0.4 eq. in degassed DCM) was added and the mixture agitated for 30 min under an inert atmosphere. The resin was washed sequentially with DCM, DMF, 0.5% w/v sodium dithiocarbamate/DMF and methanol (3 x 2 min), and the cycle repeated twice more. The terminal Fmoc was then deprotected as described above. Cyclization was performed in two cycles of 24 hr, using PyAOP (4 eq.) and DIEA (8 eq.) dissolved in 0.8M LiCl/DMF, followed by washes with DCM and DMF (3 x 2 min).

The cyclized peptide was deprotected and cleaved off the resin by treatment with a TFA/water/TIPS mixture (95:2.5:2.5) for 2 hr. The resin was then washed twice with TFA, and the combined cleavage mixture concentrated under vacuum. The resulting viscous mix was added dropwise to ice-cold diethyl ether, then the precipitated peptide was isolated by centrifugation and washed two more times with ether. The pellet containing the pellet was air-dried, taken up in deionized water, and lyophilized to obtain the final product.

The identity of the peptide was confirmed using LC/MS and 1D ^{1}H NMR. For the former, a small quantity of peptide was dissolved in 1:1 v/v acetonitrile/water and run at 1 ml/min using water/acetonitrile/TFA gradients between 95:5:0.1 and 5:95:0.1. For the latter, the peptide was mixed with 30% w/v NaOD/D_2O.

2.2.2 Peptide nanotube assembly

We assembled nanotubes of EA_4 by inducing a pH change. The lyophilized cyclic peptide was mixed with deionized water at a concentration of 2 mg/ml in a glass vial, then dissolved completely using a minimum of 1M NaOH. One tenth the volume of TFA was added to this solution dropwise with stirring, and the vial was capped and left to stir at room temperature for 24 hr. Precipitation occurred immediately on TFA addition, and a milky suspension formed overnight. This suspension was spun down to isolate the peptide nanotubes, which were washed once or twice more with deionized water till a suspension of the crystals was no longer acidic. The water suspension of nanotubes was flash frozen in liquid nitrogen and lyophilized.

2.2.3 Peptide nanotube characterization

To investigate the stability of nanotubes in various solvents, lyophilized EA_4 nanotubes were resuspended at 1 mg/ml in 0.1X Dulbecco's phosphate-buffered saline (DPBS), 1X DPBS or deionized water, at pH 4, 5.5 or 7. All solvents were supplemented with 100 mg/ml Ca^{2+} and Mg^{2+}. Suspensions were vortexed and left to stand for a week at room temperature.

For sonication experiments, 1 mg/ml of nanotube suspension (in deionized water, pH 7) was sonicated in a Branson 2510 sonicator bath (100 W, 42 kHz) at 40°C for 1 hr. Transmission electron microscopy (TEM) images were obtained on a JEOL JEM-1400 TEM operating at 80 kV. Sample solutions were vortexed and loaded onto formvar/carbon film-supported copper grids (Electron Microscopy Sciences) that were hydrophilized under glow discharge. Excess solution was blotted off and the grids stained with 1% w/v uranyl formate for imaging. For scanning electron microscopy (SEM), sample solutions were placed onto glass cover slips, air-dried, then coated with Au and imaged on a Zeiss Supra55VP FESEM at 5 kV.

2.3 Results

2.3.1 Formation of cyclic peptide nanotubes

Cyclo-[(Glu-*D*-Ala)$_4$] (EA_4) was synthesized and cyclized on-resin using solid-state peptide synthesis. Figures 2-1 and 2-2 show ^{1}H NMR and LC/MS spectra of the crude peptide respectively. The NMR spectrum corresponds well with previously published results for EL_4.[26] Because the peptide is highly charged, it eluted with the void fraction on HPLC (Figure 2-2). A small fraction of peptide (15-25%) eluted at a later time point, which we attributed to self-assembly that occurred in the acidic ~~flow solvent~~ mobile phase. Because both MS and ^{1}H NMR spectra reveal the crude product to be relatively pure, we proceeded to use the crude peptide for our experiments without further purification.

^{1}H NMR (NaOD, 400 MHz): δ 0.3 (m, 3H), δ 0.76 (m, 1H), δ 0.97 (m, 1H), δ 1.16 (m, 2H), δ 3.1 (m, 1H), δ 3.15 (m, 1H)

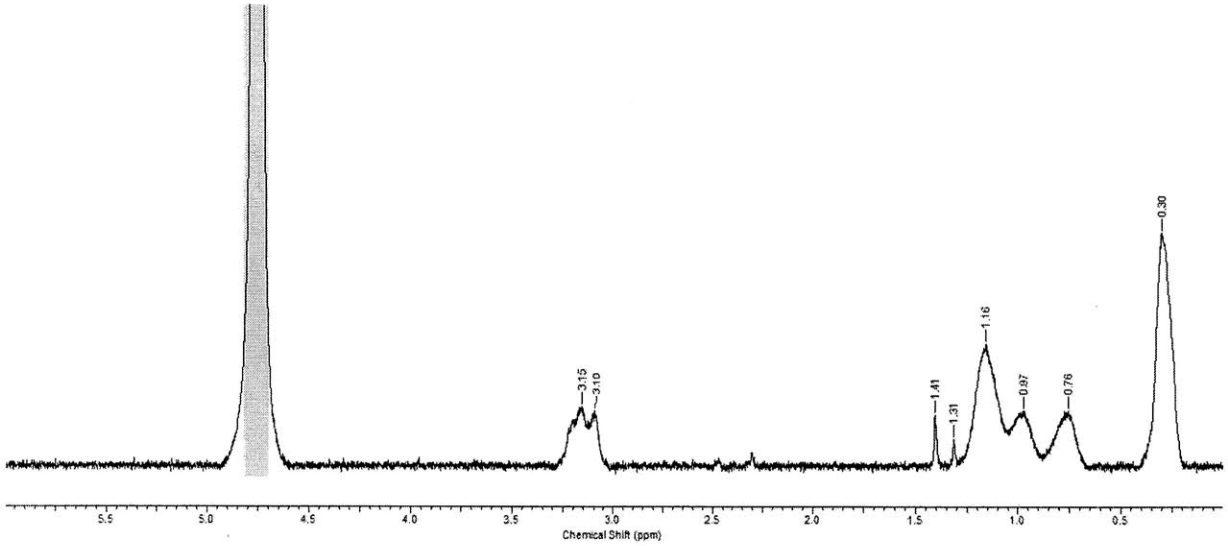

Figure 2-1: ^{1}H NMR of cyclo-[(Glu-*D*-Ala)$_4$] (EA_4).

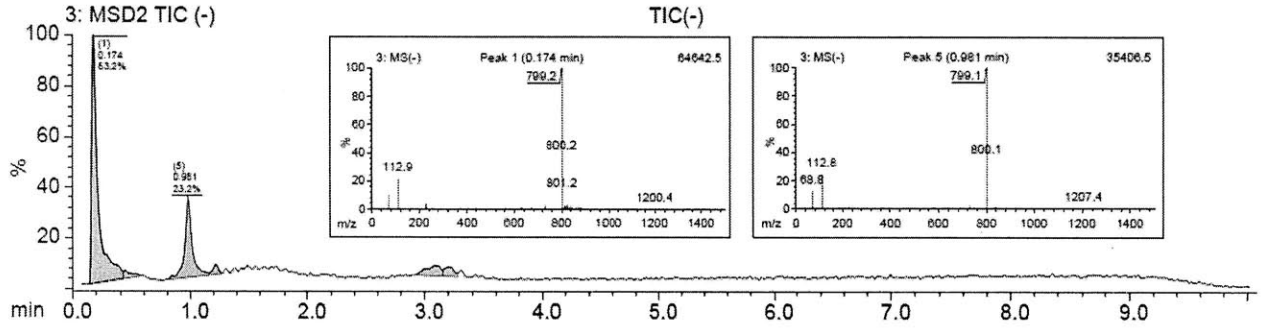

Figure 2-2: LC/MS spectra of cyclo-[(Glu-*D*-Ala)$_4$] (EA_4). Main panel shows the HPLC spectrum, while the insets show mass spectroscopy (MS) spectra corresponding to Peaks 1 and 5 on the main spectrum.

EA_4 nanotubes were obtained via pH-triggered self-assembly. The tubes were washed and flash-frozen in liquid nitrogen prior to lyophilization to prevent splintering due to the buildup of ice crystals. Because the peptide solution was stirred throughout the assembly process, we saw a heterogeneous population of tubular bundles, with diameters in the nanometer to micrometer range, and lengths up to 30 μm (Figure 2-3, left). To further break up the larger bundles, we left the tubes in a sonicator bath for 1 hr, which gave us smaller structures as revealed by TEM (Figure 2-3, right) and SEM (Figure 2-4).

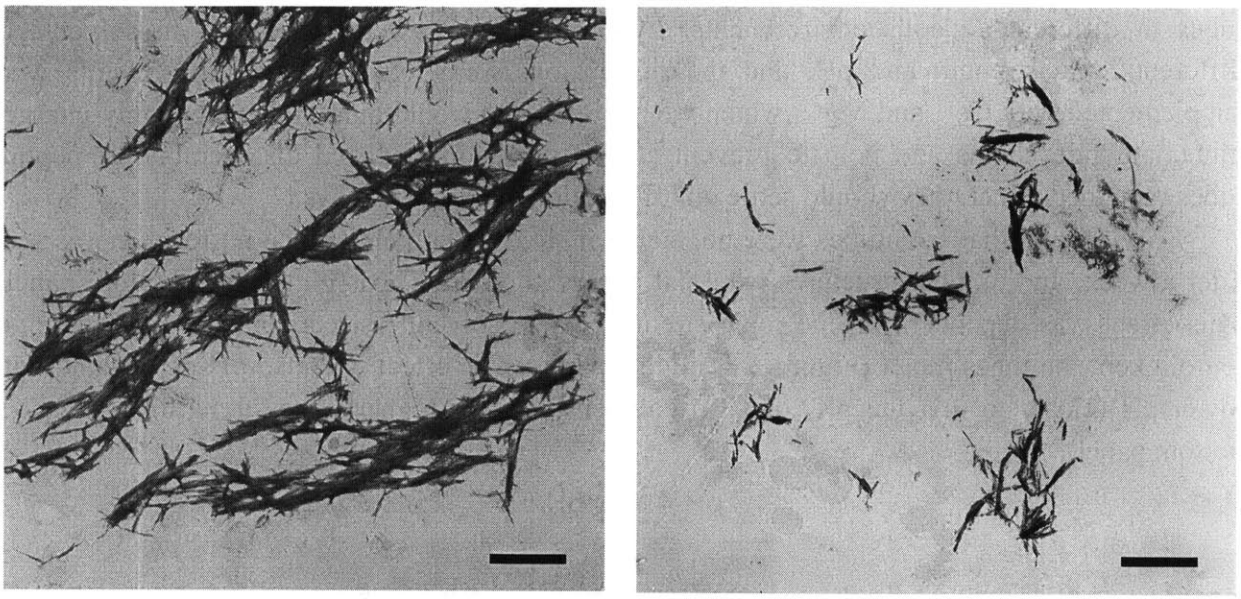

Figure 2-3: TEM images of unsonicated (left) and sonicated (right) EA_4 nanotubes. Scale bars represent 2 μm.

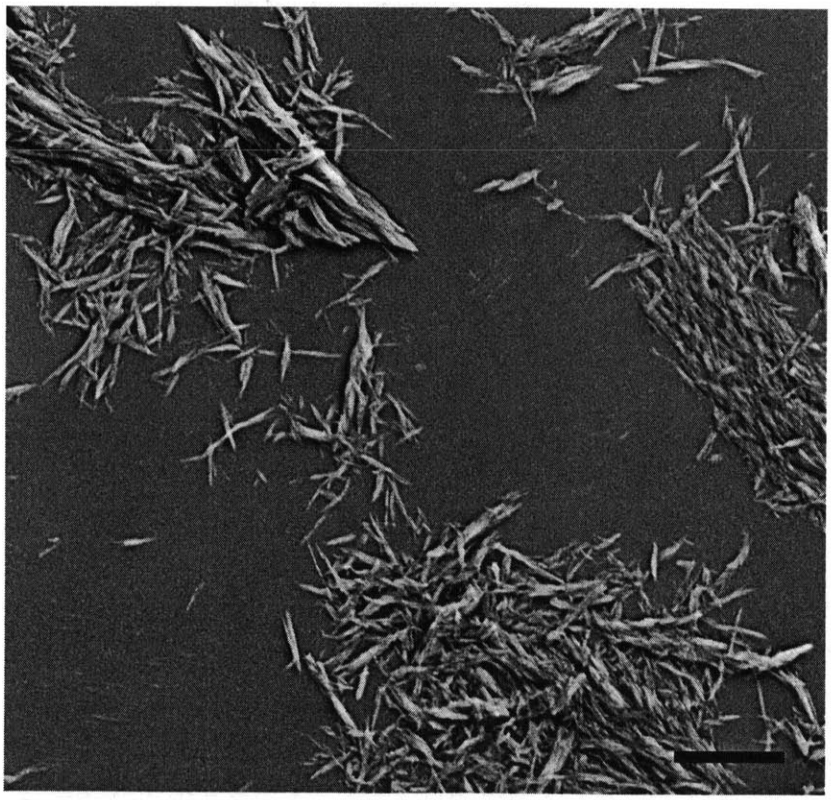

Figure 2-4: SEM image of sonicated EA_4 nanotubes. Scale bar represents 2 μm.

2.3.2 Nanotube stability in aqueous media

Although EA_4 nanotubes can be stably dispersed in water, our preliminary experiments suggested that they might dissociate in physiological buffers, thus we tested the stability of the

tubes in different aqueous environments. Lyophilized tubes were suspended in solvents of different ionic strength and pH, and the suspensions were left to stand. All solvents were supplemented with Ca^{2+} and Mg^{2+}, which we hypothesized would bind to the negatively-charged glutamate side chains and help to prevent charge repulsion-mediated disassembly. If peptide tubes remained intact, they should settle out of solution over several days.

We found that EA_4 tubes were not stable in 1X PBS at pH 7, since no residue was seen after a week, and tubular structures were not observed on the TEM (Figure 2-5, bottom panel). This effect was dependent on the ionic strength of the solvent, as reducing the ionic strength tenfold kept the tubes intact (Figure 2-5, middle panel). The effect was also pH-dependent, with lower pH (closer to 4.1, the pK_a of Glu) compensating for higher ionic strength (Figure 2-5, bottom panel).

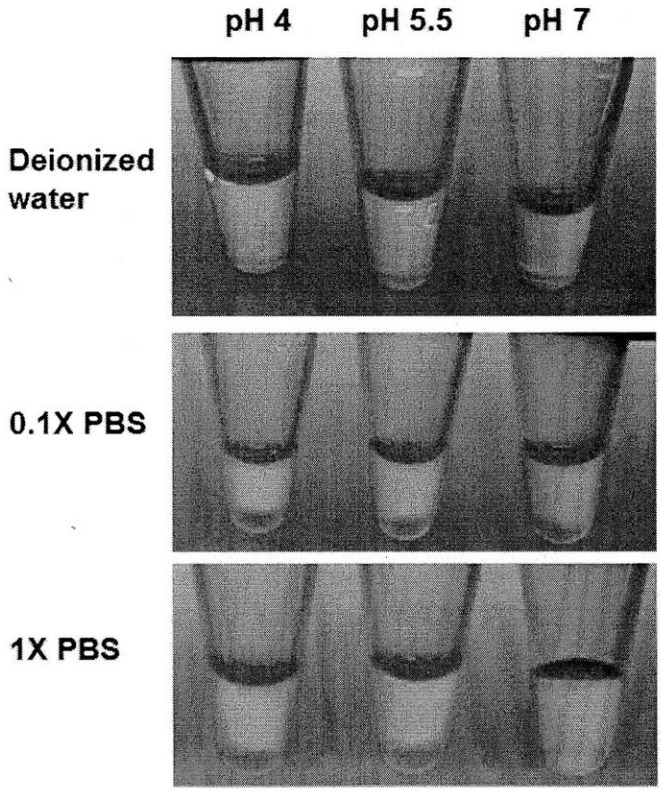

Figure 2-5: Stability of EA_4 nanotubes in solvents of different ionic strength and pH. The Eppendorf tubes contain the same concentration of peptide.

2.4 Discussion

The cyclic peptide EA_4 had several features that appealed to us. The charged Glu side chain allowed fairly rapid self-assembly using a pH trigger; the hydrophilic side chain also helped EA_4 nantubes to stay dispersed in aqueous solvents and facilitated their interaction with a range of hydrophilic polymers. Further, one or several of the Glu residues could be functionalized without affecting the mode of assembly of the peptide. Previous work with charged or hydrophilic D,L-cylic peptides mostly used vapor equilibration to assemble nanotubes,

but this slow process allowed individual tubes to aggregate into large microcrystals.[9,26,46,47] We anticipated that a more rapid titration of pH, combined with continuous stirring of the peptide mixture, would prevent extensive crystallization. This assembly process gave us a spread of tubular dimensions, although large micron-sized crystals were still evident, a result of lateral hydrogen bonding between Glu side chains of adjacent tubes. Breaking up these microcrystals was imperative to obtain a more even dispersion of tubes within the hydrogel matrix, and also to maximize the surface area available for interaction with the polymer.

Ultrasonication is commonly employed to exfoliate bundles of carbon nanotubes to better disperse them in liquids.[50] Here we sonicated a suspension of EA_4 tubes, which gave us a more uniform tube population (Figures 2-3 and 2-4). A potential downside of sonication is that it could snap nanotubular structures, thus creating greater heterogeneity in length.[51] We saw evidence of bundle scission in our electron micrographs, but because the nanotubes tended to associate in a staggered manner to form these bundles, it was difficult to determine if the scission was cause by exfoliation of individual tubes, or snapping of longer nanotubes. Nonetheless, sonication produced structures that were less polydisperse in terms of length, which was our goal. Additional stabilizers (e.g. surfactants in the case of carbon nanotubes[50]) could be added to prevent nanotubes from re-associating. Instead of introducing a small molecule stabilizer, which might disrupt tubular assembly, we relied on the hydrogel polymer to prevent re-aggregation (this will be discussed in the next chapter). For future work, we are exploring asymmetric peptide designs that would reduce lateral interaction between tubes and avoid further need for dispersion.

The integrity of hydrogen bonded networks can be affected by the ionic strength of the solvent environment, since salts interact with polar moieties and reduce the strength of hydrogen bonds. Indeed, we found that EA_4 nanotubes dissociated in 1X PBS at pH 7 even without sonication, which was different from their behavior in water described above. The tubes were stable in 0.1X PBS at the same pH, which confirmed that tube dissociation was due to the relatively high ionic strength of 1X PBS. At pH 7, a significant proportion of the Glu side chains that are exposed to solvent would be ionized, and this concentration of negative charges along the tube surface could be partially responsible for the instability of the nanotubes. This effect is known to limit tube assembly for peptide amphiphiles, but has been overcome with the addition of multivalent ionic species to reduce charge repulsion.[52,53] We sought to reproduce this effect by using PBS supplemented with Ca^{2+} and Mg^{2+}, which we hypothesized would bridge adjacent carboxylates and reduce the tendency for disassembly in PBS. Figure 2-5 shows that disassembly occurred despite the addition of stabilizing cations. It is unlikely that cation addition added significantly to the ionic strength of the solvent, since the nanotubes remained intact in 0.1X PBS supplemented with the same quantity of Ca^{2+}/Mg^{2+}. Only by lowering the pH of the solvent were we able to overcome the effects of ionic strength on nanotube stability. We explain the effects of pH as such: At pH 7, the charged Glu side groups attracted charged species in ionic solvents like PBS, concentrating the ions in the vicinity of the nanotubes, thus disrupting the hydrogen bonds necessary for self-assembly. With a decrease in pH towards the pK_a of Glu (~4.1), the Glu side

chains became protonated and no longer interacted as avidly with the solvent ions, thus the effect of solvent ionic strength was not as pronounced. Although lower pH led to greater nanotube stability, acidic media are not compatible with biological work. Ultimately, the utility of this study was that we identified a set of solvent conditions that would most adversely affect EA_4 nanotube stability (high ionic strength, pH close to 7). This provided a means of testing how well these nanotubes get incorporated into a hydrogel matrix, since good nanotube-polymer interaction is likely to further stabilize the tubular assemblies against a destabilizing solvent environment.

3. Composite hydrogel synthesis and characterization

3.1 Introduction: Choice of hydrogel system

Since we intended to use our composite hydrogels as biological substrates, we looked for polymers that were biocompatible, bioadhesive and biodegradable. Synthetic polymer hydrogels—like those made from poly(ethylene glycol) (PEG) and poly(lactic-co-glycolic acid) (PLGA)—and many natural polymer hydrogels (e.g. alginate, chitosan, hyaluronic acid) offer tailorable mechanical properties, but they do not contain biological epitopes that enable cell adhesion or cell-mediated remodeling. Conversely, collagen, an extracellular matrix (ECM) protein, and its partially-denatured product gelatin, has natural cell-binding motifs and is cell-degradable, but forms mechanically weak gels. To enable better control of the physical properties of gelatin, van den Bulcke et al. first created gelatin methacrylate (GelMA) hydrogels by conjugating methacrylate groups to side chain amines in gelatin, then photocrosslinking the modified polymer; the degree of methacrylation determined gel mechanics.[54] The Khademhosseini group has applied these hydrogels extensively in 3D cell culture, hence showing the utility of this material as a biological substrate.[55-61]

We chose GelMA for investigation because of its biocompatibility and bioactivity, and because it contains positively-charged segments that could interact with and stabilize EA_4 nanotubes. Further, the photocrosslinking process used to form the gel is unaffected by the presence of the tubes and also very rapid (<1 min), thus avoiding phase separation of the tubes from the polymer during gelation.

3.2 Materials and Methods

3.2.1 Synthesis of GelMA hydrogel containing peptide nanotubes

Gelatin methacrylate (GelMA) with a high degree of methacrylation[56] was kindly provided by the Khademhosseini lab. To prepare the nanocomposite hydrogels, we first dissolved lyophilized GelMA in deionized water at 40°C. Lyophilized EA_4 nanotubes were resuspended in deionized water (20 mg/ml) and added to the GelMA solution to give the desired final nanotube concentration (0, 1, 2.5 and 5 mg/ml). Additional water was added as necessary to the prepolymer mix to give a 5% w/v GelMA solution. This mixture was sonicated in a Branson 2510 sonicator bath (100 W, 42 kHz) at 40°C for 1 hr. The photoinitiator 2-dimethoxy-2-phenyl-acetophenone (Irgacure 2959; Aldrich) was then added at a concentration of 0.3% w/v. The prepolymer mix (60-90 μl) was dropped onto a Teflon sheet and sandwiched using a glass coverslip and 1 mm spacers. Photocuring was performed with UV light (10 mW/cm^2, 360-480 nm) for 45 s using the OmniCure S2000 Spot UV System. Poly(ethylene glycol) diacrylate (PEGDA) hydrogels were prepared similarly, using 6 kDa PEGDA (Aldrich), 0.1% w/v Irgacure 2959 and 4 min UV cure. Gel samples were detached and incubated free-floating in water, 0.1X DPBS or 1X DPBS (supplemented with Ca^{2+} and Mg^{2+}) at room temperature for 1 week. All subsequent characterization experiments were performed on gels swollen in 1X DPBS for 24 hr.

Measurements of nanotube diameter were based on TEM images of the nanotubes, obtained as in the previous chapter. Image analysis was performed using NIH ImageJ software.

Hydrogel degradation was performed using type II collagenase (Aldrich). Gel discs containing 2.5 mg/ml nanotubes were dried (see below) and placed in 1.5 ml tubes. The discs were incubated for 24 hr at 37°C with 100 μl of 0.1X DPBS containing 0.01 mg/ml (~1 U/ml) collagenase and 0.05% w/v sodium azide (Aldrich). The solution was spotted onto glass cover slips, air-dried, and coated with gold for SEM imaging.

3.2.2 Hydrogel characterization

To dry the swollen hydrogels, the latter were flash-frozen in liquid nitrogen and lyophilized. For SEM imaging, dried gel samples containing 2.5 mg/ml nanotubes were carefully cut to reveal their cross-sections, then sputter-coated with gold for imaging.

To determine hydrogel mass swelling ratios, wet gels were lightly blotted with KimWipes to remove the water on their surface, and their wet weight (W_s) was measured. The gels were then lyophilized after being frozen in liquid nitrogen, and their dry weight (W_d) was measured. The swelling ratio was calculated as follows: $(W_s - W_d) / W_d$.

Immediately prior to mechanical testing, 8 mm-diameter discs (~1 mm thick) were punched from each swollen hydrogel with a biopsy punch. Uniaxial compression was performed on an AR-G2 rheometer (TA Instruments) with a 20 mm parallel plate geometry. The discs were compressed at a strain rate of 1 mm/min, and the compressive modulus was determined from the slope of the linear region corresponding to 5-15% strain. Dynamic shear oscillation was performed on the same instrument with an 8 mm parallel plate geometry. We first did strain sweeps to verify the linear response regime, then subjected gel discs to frequency sweeps in the range of 0.1-10 Hz, at a constant 1% strain. At least four gels per sample group were used for physical characterization experiments.

3.3 Results

3.3.1 Interaction of EA_4 nanotubes with GelMA

We sonicated EA_4 peptide nanotubes (PNT) in the presence of GelMA to obtain an even dispersion of tubes in the prepolymer mix. Although TEM imaging did not reveal an obvious GelMA coating on the tubes, measurement of distinct tubular bundles gave a 50% increase in diameter (from 14 ± 4 nm for the bare tubes to 21 ± 7 nm for the coated ones), with a shift towards larger diameters in the presence of GelMA (Figure 3-1). It is possible that the presence of the polymer somehow prevented effective breaking apart of tubular clusters during sonication, but this is unlikely given that we did not observe large microcrystals in the GelMA-PNT sample.

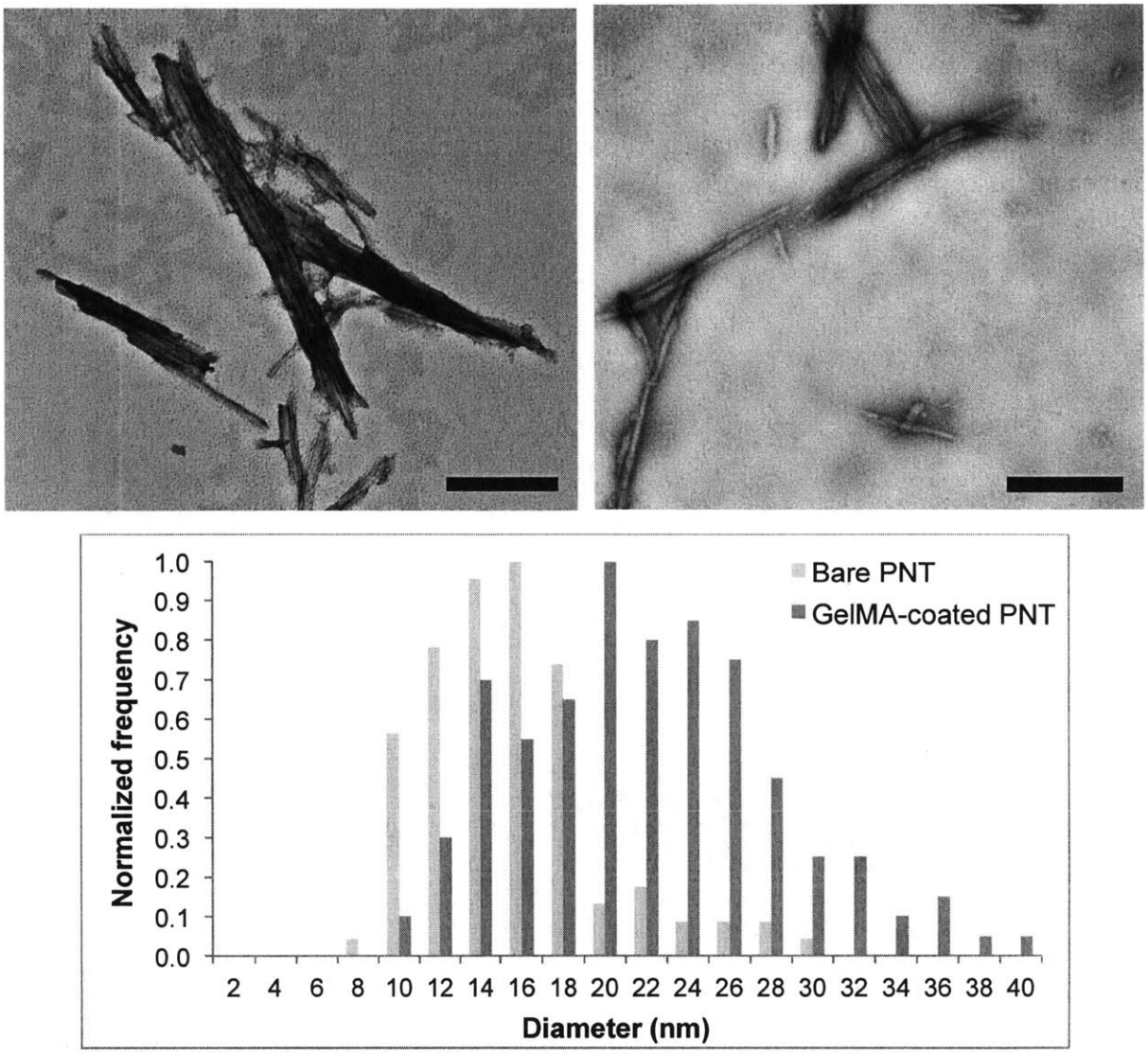

Figure 3-1: EA_4 peptide nanotubes (PNT) following mixing with GelMA. TEM images of bare PNT (above left) and GelMA-coated PNT (above right). Scale bar represents 500 nm. Bottom panel shows that diameter distribution of the two groups of nanotubes, measured using the TEM images.

5% GelMA hydrogels containing 0.25% w/v nanotubes were synthesized by photopolymerizing the macromer. The composite gels were left to swell for a week in different solvents to evaluate the stability of the nanotubes within the polymer matrix. There was no apparent change in gel opacity in water, but in ionic solvents we observed a gradual decrease in gel opacity, which occurred over several hours for gels in 1X PBS, and over several days for gels in 0.1X PBS (Figure 3-2, left panel). The dependence on ionic strength suggested that this change could be a result of tubular disassembly. For comparison, we synthesized 5% PEGDA hydrogels containing the same concentration of nanotubes; PEG was chosen since it lacked any chemical groups that could interact specifically with EA_4. Whereas the PEGDA-EA_4 composite hydrogels remained opaque in water, they rapidly turned transparent when swollen in 1X PBS,

indicating rapid nanotube disassembly (Figure 3-2, right panel). Tubular disassembly probably also occurred to EA_4 embedded in GelMA, although to a lesser extent. To show that nanotubes were still present in the composite hydrogel swollen in 1X PBS, gels containing 2.5% peptide were digested with collagenase. The digest contained tubular aggregates as seen on both phase contrast microscopy and SEM (Figure 3-3).

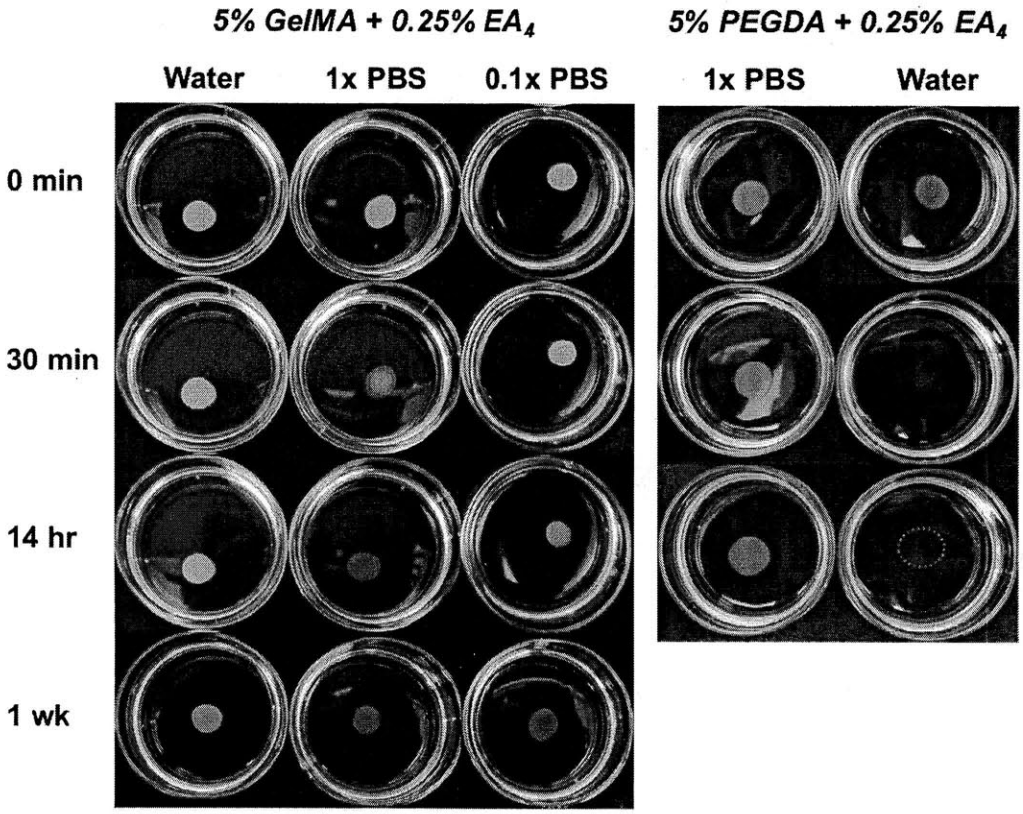

Figure 3-2: Effect of swelling medium on EA_4 in different nanocomposite hydrogels. The dotted circle on the left panel identifies the position of the transparent PEGDA gel disc.

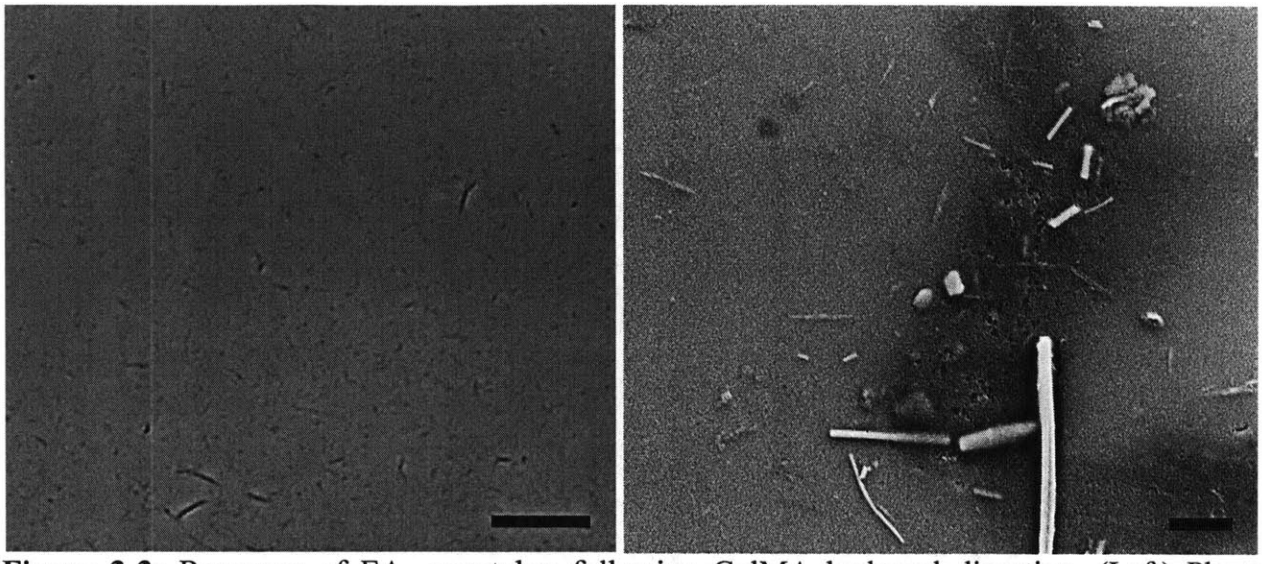

Figure 3-3: Recovery of EA_4 nanotubes following GelMA hydrogel digestion. (Left) Phase contrast image; scale bar represents 20 μm. Arrows point to the larger tubular aggregates. (Right) SEM image; scale bar represents 2 μm.

The addition of EA_4 nanotubes did not alter the porosity of the GelMA hydrogel significantly, as pore sizes remained in the 10-20 μm range. Pore walls also appeared smooth with no evidence of aggregated nanotubular structures (Figure 3-4). Closer examination of cross-sections of composite hydrogels revealed areas where the ends of peptide nanotubes were clearly visible, thus showing that the tubes were firmly embedded in the hydrogel matrix (Figure 3-5).

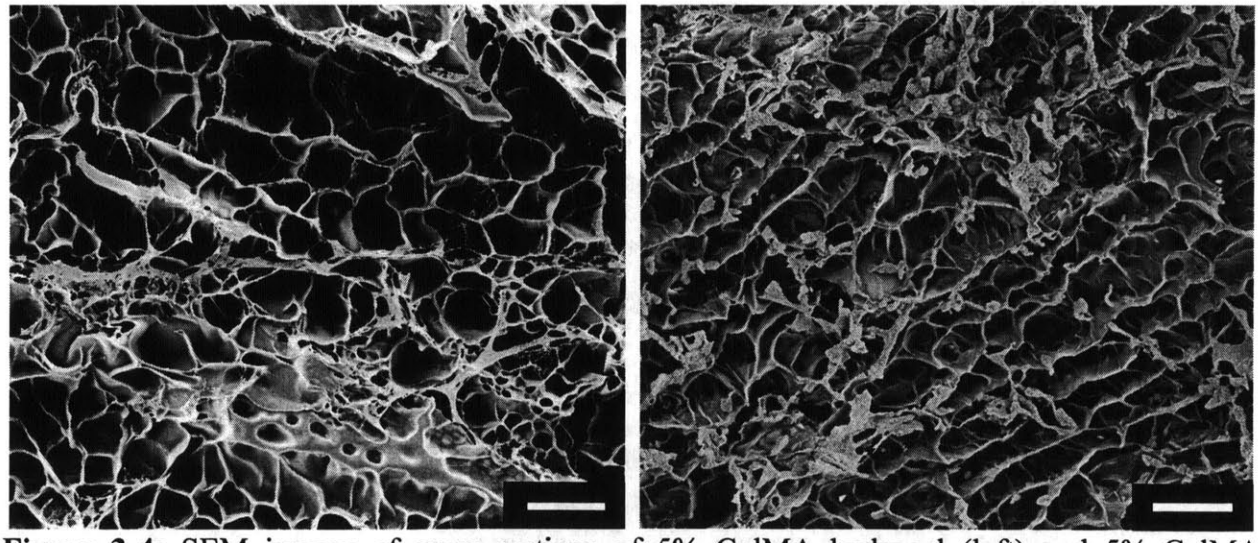

Figure 3-4: SEM images of cross sections of 5% GelMA hydrogel (left) and 5% GelMA hydrogel containing 0.5% EA_4 nanotubes (right). Scale bar represents 20 μm.

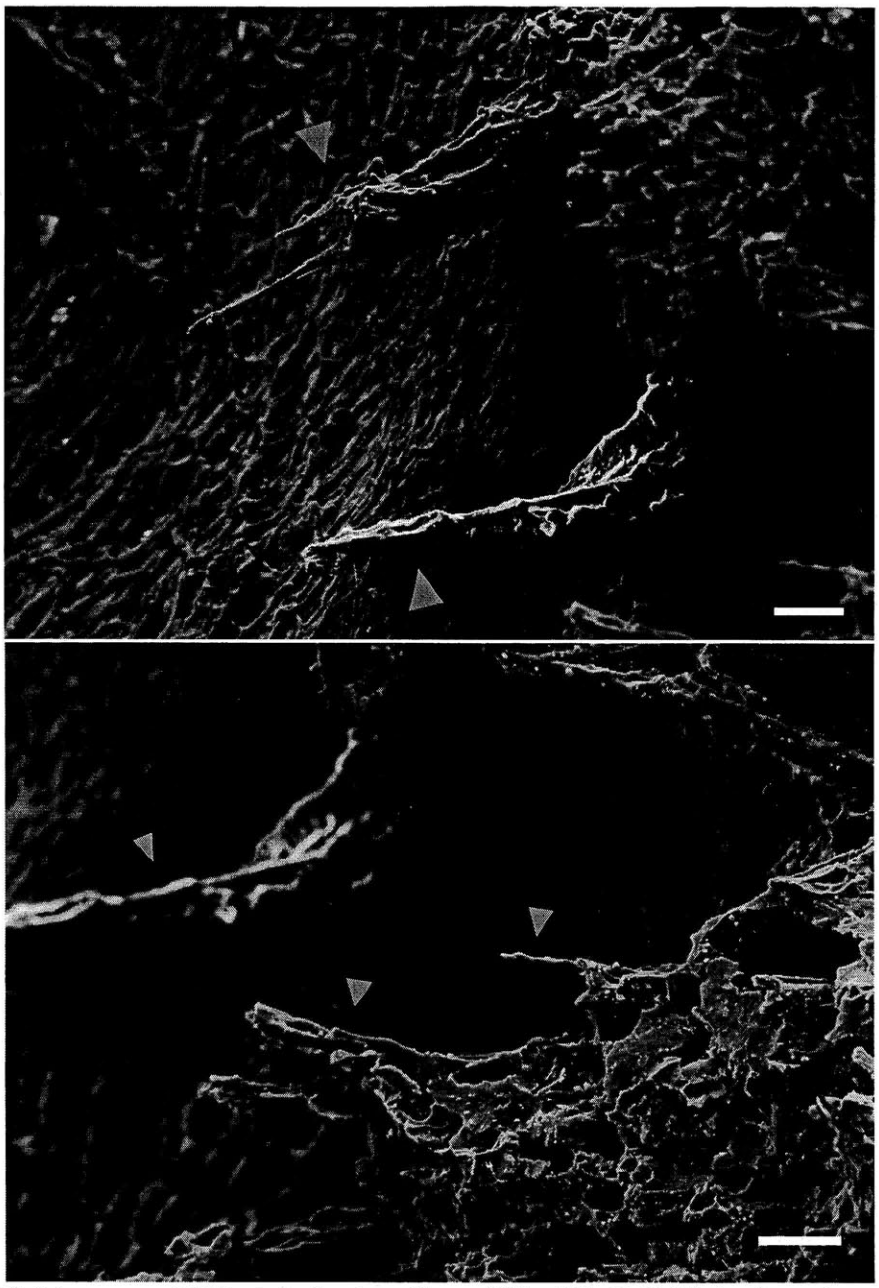

Figure 3-5: SEM images of EA_4 tubular bundles within 5% GelMA hydrogels containing 0.5% peptide. Red arrows point to the bundles. Scale bar represents 10 μm.

3.3.2 Mechanical and swelling properties of composite hydrogel

We wanted to investigate how the addition of EA4 peptide nanotubes affected the physical properties of GelMA hydrogels; 5% GelMA containing 0, 0.1, 0.25 and 0.5% w/v nanotubes were used for tests of gel swelling ratio, compressive modulus and oscillatory shear parameters. There were no apparent differences in swelling ratio of the composite gels even at high peptide concentrations, which was consistent with our findings for gel porosity (Figure 3-6, left). 5% GelMA hydrogels were fairly weak (compressive modulus = 3.4 ± 0.4 kPa). The addition of nanotubes produced a small but statistically significant increase in compressive

modulus (4.5 ± 0.5 kPa for 0.1% composite gels, 4.8 ± 0.2 kPa for 0.25% gels), although the increase was not observed at high peptide concentrations (Figure 3-6, right). This difference was very modest compared to the threefold increase in modulus reported for composite GelMA-CNT hydrogels. Rheological studies showed that the storage (*G'*) and loss moduli (*G"*) of both control and nanocomposite gels were constant at lower frequencies, the magnitude of *G'* being consistent with what was observed for the compressive modulus. Both *G'* and *G"* increased at higher frequencies (> 1 Hz), but the magnitude of increase was much more prominent with *G'* of the composite hydrogels (Figure 3-7).

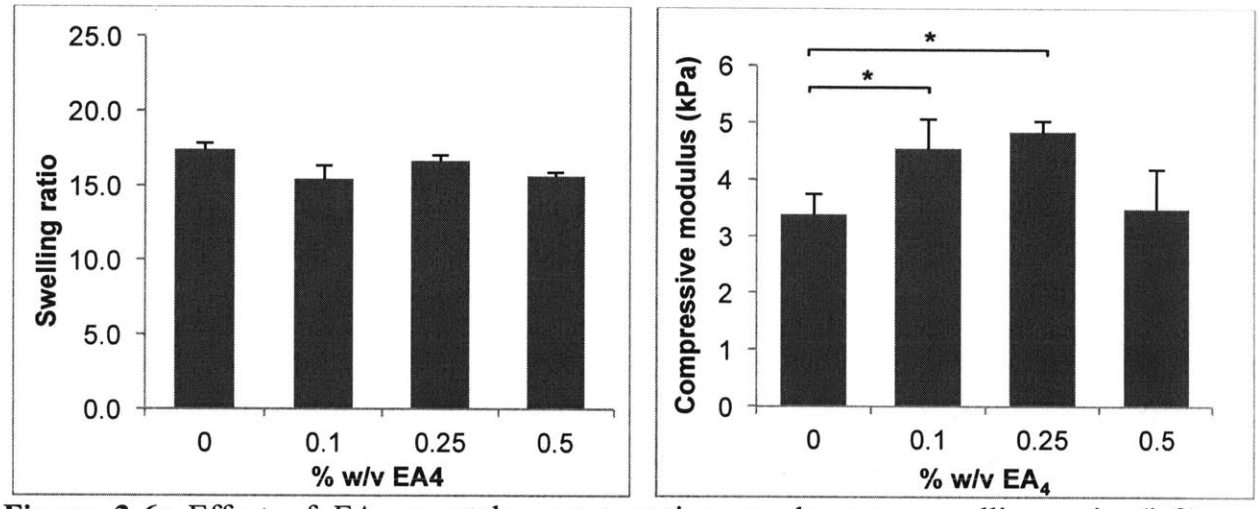

Figure 3-6: Effect of EA_4 nanotube concentration on the mass swelling ratio (left) and compressive modulus (right) of GelMA nanocomposite hydrogels. $*p < 0.05$.

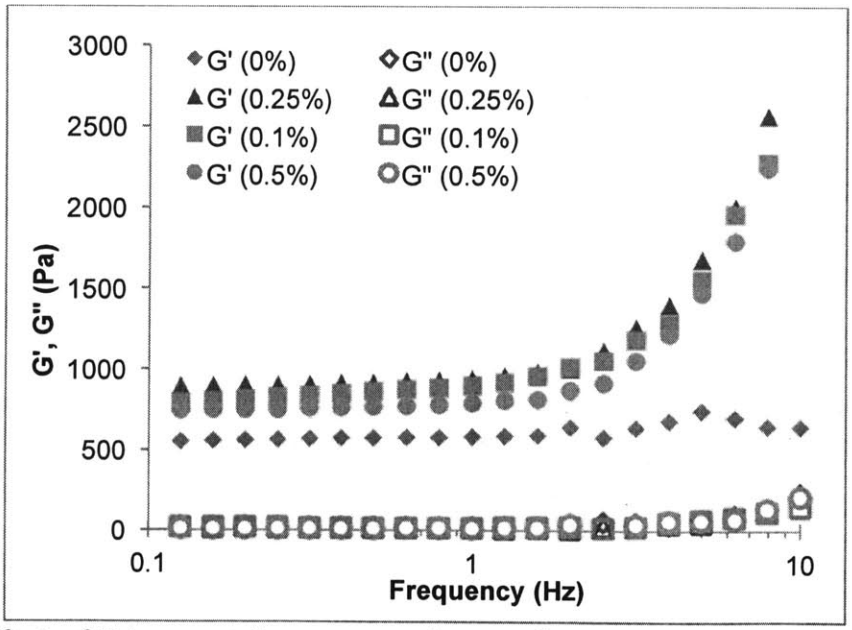

Figure 3-7: Effect of EA_4 nanotube concentration on the storage and loss moduli of GelMA nanocomposite hydrogels.

3.4 Discussion

Our characterization of the nanocomposite hydrogels focused on determining the extent of functional integration of EA_4 nanotubes within the hydrogel matrix. GelMA was chosen because it has properties that complemented EA_4. Specifically, we anticipated that its hydrophilic and positively charged domains would interact with the Glu side groups on EA_4 and act to stabilize the tubes in solution; this indeed manifested as an increase in tube diameter following mixing and sonication with GelMA (Figure 3-1). The rapid gelation of the polymer following UV exposure ensured that tubes were evenly distributed within the hydrogel, and we saw no distinct inhomogeneities in the hydrogels either visually (Figure 3-2) or on SEM (Figures 3-4 and 3-5). Where tubes were visible in hydrogel cross-sections, they appeared to be coated in a film of polymer (Figure 3-5), thus we were certain that there was good nanotube-matrix interfacing.

We chose to swell the composite hydrogels in pH 7 1X PBS to look at the stability of the nanotubes in the hydrogel. PEGDA composites completely lost their opacity in this medium, which was expected since PEG had no chemical groups that could properly interface with and reduce solvent exposure of EA_4 nanotubes (Figure 3-2). With GelMA composites, we observed some loss of opacity, which implied that not all the tubes were fully embedded in the matrix and thus shielded from the high ionic strength solvent. Collagenase digests of these composites showed that they still contained a significant quantity of tubular assemblies, although we could not quantify the proportion of tubes that dissociated during swelling.

The presence of the nanotubes did not significantly affect the porosity or the swelling characteristics of the gels (Figures 3-4 and 3-6). The majority of the tubular bundles were much smaller than the 10-20 μm average pore size of the control (0% peptide) hydrogels, so we expected them to be embedded in the pore walls. The tubes were also hydrophilic and would not have limited water uptake.

Similar composite hydrogel systems that have been constructed using nanotubular particles as fillers showed an enhancement in gel stiffness as filler content increased (typically two- to three-fold, but in some systems more than tenfold).[34,35,43,44,62] We saw a more moderate increase in gel stiffness using compressive testing (Figure 3-6). This could be caused by buckling of the tubes at high strain; stripping of the GelMA layer around the tubes during gel compression, which would reduce the functional interface between nanotube and gel matrix; the heterogeneity in the dimensions of the tubes being used; or the lack of an extensive tubular network to evenly distribute the stress. At the highest peptide concentration tested (0.5% w/v), there appeared to be no improvement in gel stiffness, perhaps because the tubes were being forced against each other and were splintering as a result. We would need to incorporate tube bundles of different dimensions to draw more concrete conclusions regarding their effect on gel mechanics.

Rheological experiments provided more convincing evidence that the tubes were interacting with GelMA. There was a dramatic increase in storage modulus (Figure 3-7) at higher frequencies for all peptide concentrations used. We believe that the tubes embedded in the gel

were obstructing relaxation of the GelMA network at high oscillatory frequencies, giving rise to an apparent stiffening effect.

4. General conclusions

4.1 Overview of current progress

D,L-cyclic peptides (DLCP) form stiff nanotubular assemblies with surface chemistry that can be modified by changing the peptide amino acid sequence. This provides a means of creating nanotubes with interesting physical and chemical properties. Our goal in this project was to create a platform that would exploit the structural features and chemical versatility of DLCP nanotubes to create biological scaffolds with novel properties. We chose gelatin methacrylate (GelMA) as our hydrogel scaffold for its biocompatibility and biodegradability, and also for its rapid gelation on UV exposure. For this initial study, we focused on nanotubes assembled from cyclo-[(Glu-*D*-Ala)$_4$] (EA_4), which had negatively charged Glu side chains that could interact with domains in gelatin, and also provide a chemical handle for further functionalization.

We successfully prepared nanocomposite GelMA hydrogels containing EA_4 nanotubes. The polymer was shown to coat the tubes, which enabled functional integration with the gel matrix, and stabilized the tubes against relatively high ionic strength solvents like 1X PBS. The presence of the nanotubes provided a modest increase to the compressive modulus of the hydrogel, without reducing its porosity or swelling capacity.

4.2 Future directions

Our composite system is not yet optimized. We are currently exploring ways to covalently link the nanotubes to the hydrogel, either during or post-polymerization, to increase functional integration of the two components, and provide a greater degree of mechanical reinforcement. We are also looking at other cyclic peptide designs that would minimize aggregation in aqueous solutions and provide greater stability in physiological buffers. Although GelMA was an appropriate choice for our current system, we might use other polymers if they are more relevant to future peptide designs.

To demonstrate the utility of our platform for introducing new properties to hydrogels, we will eventually be employing functionalized nanotubes. We are particularly interested in creating conductive systems based on nanotube "wires", and also biomineralized matrices for tissue engineering. Co-incorporation of multiple peptide nanotubes could potentially expand the functionality of our composite system. Finally, we would need to determine the biocompatibility of these nanocomposite systems to show that they are suitable as biological substrates.

References

1 Ikeda, T., Oosawa, K. & Hotani, H. Self-assembly of the filament capping protein, FliD, of bacterial flagella into an annular structure. *Journal of Molecular Biology* **259**, 679-686, doi:10.1006/jmbi.1996.0349 (1996).

2 Wang, X., Hammer, N. D. & Chapman, M. R. The molecular basis of functional bacterial amyloid polymerization and nucleation. *Journal of Biological Chemistry* **283**, 21530-21539, doi:10.1074/jbc.M800466200 (2008).

3 Adler-Abramovich, L. *et al.* Thermal and chemical stability of diphenylalanine peptide nanotubes: Implications for nanotechnological applications. *Langmuir* **22**, 1313-1320, doi:10.1021/la052409d (2006).

4 Kol, N. *et al.* Self-assembled peptide nanotubes are uniquely rigid bioinspired supramolecular structures. *Nano Letters* **5**, 1343-1346, doi:10.1021/nl0505896 (2005).

5 Vauthey, S., Santoso, S., Gong, H. Y., Watson, N. & Zhang, S. G. Molecular self-assembly of surfactant-like peptides to form nanotubes and nanovesicles. *Proceedings of the National Academy of Sciences of the United States of America* **99**, 5355-5360, doi:10.1073/pnas.072089599 (2002).

6 Matsui, H. & Douberly, G. E. Organization of peptide nanotubes into macroscopic bundles. *Langmuir* **17**, 7918-7922, doi:10.1021/la010910+ (2001).

7 Hartgerink, J. D., Beniash, E. & Stupp, S. I. Peptide-amphiphile nanofibers: A versatile scaffold for the preparation of self-assembling materials. *Proceedings of the National Academy of Sciences* **99**, 5133-5138, doi:10.1073/pnas.072699999 (2002).

8 De Santis, P., Morosetti, S. & Rizzo, R. Conformational Analysis of Regular Enantiomeric Sequences. *Macromolecules* **7**, 52-58, doi:10.1021/ma60037a011 (1974).

9 Ghadiri, M. R., Granja, J. R., Milligan, R. A., McRee, D. E. & Khazanovich, N. Self-assembling Organic Nanotubes based on a Cyclic Peptide Architecture. *Nature* **366**, 324-327, doi:10.1038/366324a0 (1993).

10 Seebach, D. *et al.* Cyclo-beta-peptides: Structure and tubular stacking of cyclic tetramers of 3-aminobutanoic acid as determined from powder diffraction data. *Helvetica Chimica Acta* **80**, 173-182, doi:10.1002/hlca.19970800116 (1997).

11 Clark, T. D., Buehler, L. K. & Ghadiri, M. R. Self-assembling cyclic beta(3)-peptide nanotubes as artificial transmembrane ion channels. *J. Am. Chem. Soc.* **120**, 651-656, doi:10.1021/ja972786f (1998).

12 Amorín, M., Castedo, L. & Granja, J. R. New Cyclic Peptide Assemblies with Hydrophobic Cavities: The Structural and Thermodynamic Basis of a New Class of Peptide Nanotubes. *J. Am. Chem. Soc.* **125**, 2844-2845, doi:10.1021/ja0296273 (2003).

13 Amorín, M., Castedo, L. & Granja, J. R. Folding Control in Cyclic Peptides through N-Methylation Pattern Selection: Formation of Antiparallel β-Sheet Dimers, Double Reverse Turns and Supramolecular Helices by 3α,γ Cyclic Peptides. *Chemistry – A European Journal* **14**, 2100-2111, doi:10.1002/chem.200701059 (2008).

14 Horne, W. S., Stout, C. D. & Ghadiri, M. R. A Heterocyclic Peptide Nanotube. *J. Am. Chem. Soc.* **125**, 9372-9376, doi:10.1021/ja034358h (2003).

15 Chapman, R., Danial, M., Koh, M. L., Jolliffe, K. A. & Perrier, S. Design and properties of functional nanotubes from the self-assembly of cyclic peptide templates. *Chemical Society Reviews* **41**, 6023-6041 (2012).

16 Clark, T. D. *et al.* Cylindrical beta-sheet peptide assemblies. *J. Am. Chem. Soc.* **120**, 8949-8962, doi:10.1021/ja981485i (1998).
17 Clark, T. D. & Ghadiri, M. R. SUPRAMOLECULAR DESIGN BY COVALENT CAPTURE - DESIGN OF A PEPTIDE CYLINDER VIA HYDROGEN-BOND-PROMOTED INTERMOLECULAR OLEFIN METATHESIS. *J. Am. Chem. Soc.* **117**, 12364-12365, doi:10.1021/ja00154a051 (1995).
18 Fernandez-Lopez, S. *et al.* Antibacterial agents based on the cyclic d,l-[alpha]-peptide architecture. *Nature* **412**, 452-455 (2001).
19 Ghadiri, M. R., Granja, J. R. & Buehler, L. K. Artificial transmembrane ion channels from self-assembling peptide nanotubes. *Nature* **369**, 301-304 (1994).
20 Granja, J. R. & Ghadiri, M. R. Channel-Mediated Transport of Glucose across Lipid Bilayers. *J. Am. Chem. Soc.* **116**, 10785-10786, doi:10.1021/ja00102a054 (1994).
21 Sánchez-Quesada, J., Sun Kim, H. & Ghadiri, M. R. A Synthetic Pore-Mediated Transmembrane Transport of Glutamic Acid. *Angewandte Chemie International Edition* **40**, 2503-2506, doi:10.1002/1521-3773(20010702)40:13<2503::aid-anie2503>3.0.co;2-e (2001).
22 Motesharei, K. & Ghadiri, M. R. Diffusion-Limited Size-Selective Ion Sensing Based on SAM-Supported Peptide Nanotubes. *J. Am. Chem. Soc.* **119**, 11306-11312, doi:10.1021/ja9727171 (1997).
23 Ashkenasy, N., Horne, W. S. & Ghadiri, M. R. Design of Self-Assembling Peptide Nanotubes with Delocalized Electronic States. *Small* **2**, 99-102, doi:10.1002/smll.200500252 (2006).
24 Fujimura, F. & Kimura, S. Columnar Assembly Formation and Metal Binding of Cyclic Tri-β-peptides Having Terpyridine Ligands. *Organic Letters* **9**, 793-796, doi:10.1021/ol0629622 (2007).
25 Hartgerink, J. D., Clark, T. D. & Ghadiri, M. R. Peptide nanotubes and beyond. *Chemistry-a European Journal* **4**, 1367-1372, doi:10.1002/(sici)1521-3765(19980807)4:8<1367::aid-chem1367>3.0.co;2-b (1998).
26 Hartgerink, J. D. *Self-assembling peptide nanotubes* PhD thesis, The Scripps Research Institute, (1999).
27 Brea, R. J. *et al.* Electron transfer in Me-blocked heterodimeric alpha,gamma-peptide nanotubular donor-acceptor hybrids. *Proceedings of the National Academy of Sciences of the United States of America* **104**, 5291-5294, doi:10.1073/pnas.0609506104 (2007).
28 Couet, J., Samuel, J. D. J. S., Kopyshev, A., Santer, S. & Biesalski, M. Peptide–Polymer Hybrid Nanotubes. *Angewandte Chemie International Edition* **44**, 3297-3301, doi:10.1002/anie.200462993 (2005).
29 Gokhale, R., Couet, J. & Biesalski, M. In situ cross-linking of the shell of self-assembled peptide nanotubes. *physica status solidi (a)* **207**, 878-883, doi:10.1002/pssa.200983314 (2010).
30 Lau, C., Cooney, M. J. & Atanassov, P. Conductive Macroporous Composite Chitosan−Carbon Nanotube Scaffolds. *Langmuir* **24**, 7004-7010, doi:10.1021/la8005597 (2008).
31 Wang, S.-F., Shen, L., Zhang, W.-D. & Tong, Y.-J. Preparation and Mechanical Properties of Chitosan/Carbon Nanotubes Composites. *Biomacromolecules* **6**, 3067-3072, doi:10.1021/bm050378v (2005).

32 Zhao, X. *et al.* Active scaffolds for on-demand drug and cell delivery. *Proceedings of the National Academy of Sciences* **108**, 67-72, doi:10.1073/pnas.1007862108 (2011).
33 Souza, G. R. *et al.* Three-dimensional tissue culture based on magnetic cell levitation. *Nat Nano* **5**, 291-296, doi:http://www.nature.com/nnano/journal/v5/n4/suppinfo/nnano.2010.23_S1.html (2010).
34 Araki, J., Yamanaka, Y. & Ohkawa, K. Chitin-chitosan nanocomposite gels: reinforcement of chitosan hydrogels with rod-like chitin nanowhiskers. *Polymer Journal* **44**, 713-717, doi:10.1038/pj.2012.11 (2012).
35 Dahman, Y. & Oktem, T. Optically transparent nanocomposites reinforced with modified biocellulose nanofibers. *Journal of Applied Polymer Science* **126**, E187-E195, doi:10.1002/app.36756 (2012).
36 Liu, M., Li, W., Rong, J. & Zhou, C. Novel polymer nanocomposite hydrogel with natural clay nanotubes. *Colloid and Polymer Science* **290**, 895-905, doi:10.1007/s00396-012-2588-z (2012).
37 Gaharwar, A. K., Rivera, C. P., Wu, C.-J. & Schmidt, G. Transparent, elastomeric and tough hydrogels from poly(ethylene glycol) and silicate nanoparticles. *Acta Biomaterialia* **7**, 4139-4148, doi:10.1016/j.actbio.2011.07.023 (2011).
38 Pek, Y. S., Gao, S., Arshad, M. S. M., Leck, K.-J. & Ying, J. Y. Porous collagen-apatite nanocomposite foams as bone regeneration scaffolds. *Biomaterials* **29**, 4300-4305, doi:10.1016/j.biomaterials.2008.07.030 (2008).
39 Song, J.-H., Kim, H.-E. & Kim, H.-W. Collagen-apatite nanocomposite membranes for guided bone regeneration. *Journal of Biomedical Materials Research Part B-Applied Biomaterials* **83B**, 248-257, doi:10.1002/jbm.b.30790 (2007).
40 Nudelman, F. *et al.* The role of collagen in bone apatite formation in the presence of hydroxyapatite nucleation inhibitors. *Nature Materials* **9**, 1004-1009, doi:10.1038/nmat2875 (2010).
41 Satarkar, N. S., Biswal, D. & Hilt, J. Z. Hydrogel nanocomposites: a review of applications as remote controlled biomaterials. *Soft Matter* **6**, 2364-2371, doi:10.1039/b925218p (2010).
42 Aime, C. & Coradin, T. Nanocomposites from biopolymer hydrogels: Blueprints for white biotechnology and green materials chemistry. *Journal of Polymer Science Part B-Polymer Physics* **50**, 669-680, doi:10.1002/polb.23061 (2012).
43 Dai, Q. & Kadla, J. F. Effect of Nanofillers on Carboxymethyl Cellulose/Hydroxyethyl Cellulose Hydrogels. *Journal of Applied Polymer Science* **114**, 1664-1669, doi:10.1002/app.30789 (2009).
44 Wang, S. F., Shen, L., Zhang, W. D. & Tong, Y. J. Preparation and mechanical properties of chitosan/carbon nanotubes composites. *Biomacromolecules* **6**, 3067-3072, doi:10.1021/bm050378v (2005).
45 de Mesquita, J. P., Donnici, C. L. & Pereira, F. V. Biobased Nanocomposites from Layer-by-Layer Assembly of Cellulose Nanowhiskers with Chitosan. *Biomacromolecules* **11**, 473-480, doi:10.1021/bm9011985 (2010).
46 Khazanovich, N., Granja, J. R., McRee, D. E., Milligan, R. A. & Ghadiri, M. R. Nanoscale tubular ensembles with specified internal diameters: Design of a self-assembled nanotube with a 13-angstrom pore. *J. Am. Chem. Soc.* **116**, 6011-6012, doi:10.1021/ja00092a079 (1994).

47 Hartgerink, J. D., Granja, J. R., Milligan, R. A. & Ghadiri, M. R. Self-assembling peptide nanotubes. *J. Am. Chem. Soc.* **118**, 43-50, doi:10.1021/ja953070s (1996).
48 Rovero, P., Quartara, L. & Fabbri, G. Synthesis of Cyclic-peptides on Solid Support. *Tetrahedron Lett.* **32**, 2639-2642, doi:10.1016/s0040-4039(00)78806-x (1991).
49 Sarin, V. K., Kent, S. B. H., Tam, J. P. & Merrifield, R. B. Quantitative Monitoring of Solid-phase Peptide-Synthesis by the Ninhydrin Reaction. *Anal. Biochem.* **117**, 147-157, doi:10.1016/0003-2697(81)90704-1 (1981).
50 Hilding, J., Grulke, E. A., Zhang, Z. G. & Lockwood, F. Dispersion of carbon nanotubes in liquids. *J. Dispersion Sci. Technol.* **24**, 1-41, doi:10.1081/dis-120017941 (2003).
51 Pagani, G., Green, M. J., Poulin, P. & Pasquali, M. Competing mechanisms and scaling laws for carbon nanotube scission by ultrasonication. *Proceedings of the National Academy of Sciences of the United States of America* **109**, 11599-11604, doi:10.1073/pnas.1200013109 (2012).
52 Zou, D. *et al.* Effects of Hydrophobicity and Anions on Self-Assembly of the Peptide EMK16-II. *Biopolymers* **93**, 318-329, doi:10.1002/bip.21340 (2010).
53 Bakota, E. L., Wang, Y., Danesh, F. R. & Hartgerink, J. D. Injectable Multidomain Peptide Nanofiber Hydrogel as a Delivery Agent for Stem Cell Secretome. *Biomacromolecules* **12**, 1651-1657, doi:10.1021/bm200035r (2011).
54 Van den Bulcke, A. I. *et al.* Structural and rheological properties of methacrylamide modified gelatin hydrogels. *Biomacromolecules* **1**, 31-38, doi:10.1021/bm990017d (2000).
55 Benton, J. A., DeForest, C. A., Vivekanandan, V. & Anseth, K. S. Photocrosslinking of Gelatin Macromers to Synthesize Porous Hydrogels That Promote Valvular Interstitial Cell Function. *Tissue Eng. Part A* **15**, 3221-3230, doi:10.1089/ten.tea.2008.0545 (2009).
56 Nichol, J. W. *et al.* Cell-laden microengineered gelatin methacrylate hydrogels. *Biomaterials* **31**, 5536-5544, doi:10.1016/j.biomaterials.2010.03.064 (2010).
57 Shin, H., Olsen, B. D. & Khademhosseini, A. The mechanical properties and cytotoxicity of cell-laden double-network hydrogels based on photocrosslinkable gelatin and gellan gum biomacromolecules. *Biomaterials* **33**, 3143-3152, doi:10.1016/j.biomaterials.2011.12.050 (2012).
58 Gauvin, R. *et al.* Microfabrication of complex porous tissue engineering scaffolds using 3D projection stereolithography. *Biomaterials* **33**, 3824-3834, doi:10.1016/j.biomaterials.2012.01.048 (2012).
59 Ramon-Azcon, J. *et al.* Gelatin methacrylate as a promising hydrogel for 3D microscale organization and proliferation of dielectrophoretically patterned cells. *Lab on a Chip* **12**, 2959-2969, doi:10.1039/c2lc40213k (2012).
60 Xiao, W. *et al.* Synthesis and characterization of photocrosslinkable gelatin and silk fibroin interpenetrating polymer network hydrogels. *Acta Biomaterialia* **7**, 2384-2393, doi:10.1016/j.actbio.2011.01.016 (2011).
61 Aubin, H. *et al.* Directed 3D cell alignment and elongation in microengineered hydrogels. *Biomaterials* **31**, 6941-6951, doi:10.1016/j.biomaterials.2010.05.056 (2010).
62 Shin, S. R. *et al.* Carbon Nanotube Reinforced Hybrid Microgels as Scaffold Materials for Cell Encapsulation. *ACS Nano* **6**, 362-372, doi:10.1021/nn203711s (2012).